Theoretical study of dynamic effects on fusion cross sections for reactions $^{32,34,36}S + ^{204,206,208}Pb$

Jian-Mei Yang (杨健梅), Zheng-Wei Song (宋政伟), Wei-Juan Zhao (赵维娟), and Bing Wang (王兵)*
School of Physics and Microelectronics, Zhengzhou University, Zhengzhou 450001, China

(Received 12 July 2021; accepted 25 August 2021; published 7 September 2021)

The universal fusion function prescription and the empirical coupled-channel (ECC) model are used to analyze the dynamic effects on fusion cross sections for reactions $^{32,34,36}S + ^{204,206,208}Pb$. An examination of the reduced fusion functions shows that the total dynamic effects on fusion cross sections in $^{36}S + ^{204,206,208}Pb$ are almost the same as those in $^{34}S + ^{204,206,208}Pb$. Furthermore, at sub-barrier energies of the reactions $^{32,34,36}S + ^{208}Pb$, the largest enhancement of reduced fusion function is observed in the reaction $^{32}S + ^{208}Pb$. Then the enhancement of fusion cross sections due to couplings to inelastic excitation channels and neutron transfer channels with positive Q values is investigated by using the ECC model. The results show that the experimental data of the reactions $^{34,36}S + ^{204,206,208}Pb$ and $^{32}S + ^{208}Pb$ are reproduced well by the ECC model. In addition, it can be found that the effect of coupling to positive Q-value neutron transfer channels is necessary to reproduce the sub-barrier fusion data of the reaction $^{32}S + ^{208}Pb$. Furthermore, for the two reactions $^{32}S + ^{204}Pb$ and $^{32}S + ^{206}Pb$, the effects of coupling to positive Q-value neutron transfer channels are predicted to be significant. The fusion cross sections for these two reactions are also predicted.

DOI: 10.1103/PhysRevC.104.034607

I. INTRODUCTION

The heavy-ion fusion reaction has received a great amount of attention for several decades, which arises from the fact that the heavy-ion fusion reaction is not only of central importance for nucleosynthesis, but also can reveal the influence of the structure of the reacting nuclei on reaction dynamics [1,2]. The study of the fusion reaction is also of crucial importance for understanding the synthesis of superheavy nuclei [3–14] and the mechanism of reactions involving weakly bound nuclei [15,16]. Up to present, at energies near and above the Coulomb barrier, many experimental and theoretical studies have revealed a lot of important information about the fusion dynamics, such as the hindrance of fusion at deep sub-barrier energies [17–22], the influence of breakup effects on fusion [23–30], and the role of the neutron transfer (NT) channel with a positive Q value in fusion [31–34], etc.

It is well known that the measured fusion cross sections at sub-barrier energies are enhanced as compared to predictions from a single barrier penetration model. This enhancement is not only associated with coupling to inelastic excitation channels, but also likely related to coupling to positive Q-value neutron transfer (PQNT) channels. For many reaction systems with PQNT channels, an extra enhancement of sub-barrier fusion cross sections has been observed as compared with predictions only considering the coupling to inelastic excitation channels, such as $^{58}Ni + ^{64}Ni$ [23], $^{32}S + ^{94,96}Zr$ [35,36], $^{40}Ca + ^{94,96}Zr$ [37,38], $^{32}S + ^{106,108,110}Pd$ [39], $^{124,132}Sn + ^{40}Ca$ [40], $^{35}Cl + ^{130}Te$ [41], etc. In contrast, in some other experiments for reaction systems with PQNT channels [42,43], no extra enhancement was observed in the fusion cross sections at sub-barrier energies.

Theoretically, many efforts have been made to investigate the effect of coupling to PQNT channels [26,44–48]. In the quantum coupled-channel model, the coupling to the two-neutron transfer channel with a positive Q value is considered by introducing a macroscopic coupling form factor [48]. Zagrebaev has proposed a simplified semiclassical model to consider the effect of neutron transfer channels on fusion [44]. Within the quantum diffusion approach, the effect of coupling to the two-neutron transfer channel with a positive Q value is taken into account by changing the deformation parameters of the projectile and the target [45–47]. In the time-dependent Hartree-Fock method [49–55] and the quantum molecular dynamic model [56–61], effects of inelastic excitation and neutron transfer couplings are all automatically included. Although many theoretical and experimental efforts have devoted to investigate the effect of coupling to PQNT channels on fusion, the role of neutron transfer in fusion process has never been unambiguously identified.

In our previous work [62], we have developed an empirical coupled-channel (ECC) model in which a barrier weight function has been introduced to effectively take into account the coupled-channel effects. Within this model the effect of coupling to PQNT channels is simulated by broadening the barrier weight function. In Ref. [62], the ECC model has been applied to systematically investigate the fusion excitation functions of 220 reaction systems. For 89 reactions among them, the Q values for the two-neutron transfer channel are positive. For most of these 89 reaction systems, the data of the fusion cross sections have been reproduced by this ECC model.

*bingwang@zzu.edu.cn

TABLE I. Q values for one or multineutron transferring from the ground state of the target to the ground state of the projectile for $^{32,34,36}S + ^{204,206,208}Pb$.

Reaction	$Q(1n)$ (MeV)	$Q(2n)$ (MeV)	$Q(3n)$ (MeV)	$Q(4n)$ (MeV)
$^{32}S + ^{204}Pb$	0.25	4.77	2.98	5.79
$^{32}S + ^{206}Pb$	0.56	5.24	3.83	6.80
$^{32}S + ^{208}Pb$	1.27	5.95	4.85	8.01
$^{34}S + ^{204}Pb$	−1.41	1.56	−2.89	−1.94
$^{34}S + ^{206}Pb$	−1.10	2.06	−2.03	−0.92
$^{32}S + ^{208}Pb$	−0.38	2.77	−1.01	−0.29
$^{36}S + ^{204}Pb$	−4.10	−2.98	−7.35	−6.67
$^{36}S + ^{206}Pb$	−3.78	−2.48	−6.50	−5.65
$^{36}S + ^{208}Pb$	−3.06	−1.77	−5.48	−4.43

In Ref. [63], the fusion excitation functions for reactions $^{34,36}S + ^{204,206,208}Pb$ have been measured. Especially a larger enhancement of fusion cross sections at sub-barrier energies was observed in $^{34}S + ^{204,206,208}Pb$ as compared to those of $^{36}S + ^{204,206,208}Pb$, this observation was explained by a stronger coupling to the vibrational states in the reactions with ^{34}S as the projectile. It is interesting to note that the Q values of the two-neutron transfer channel, i.e., $Q(2n)$s for reactions $^{34}S + ^{204,206,208}Pb$ are positive whereas for reactions $^{36}S + ^{204,206,208}Pb$ the $Q(2n)$s are negative. The $Q(xn)$ values for these reactions are listed in Table I. Furthermore, for reactions $^{32}S + ^{204,206,208}Pb$, the $Q(2n)$s are also positive and even much larger than those of reactions with ^{34}S as the projectile. In the present paper, we will first investigate the dynamic effects on fusion cross sections for reactions $^{34,36}S + ^{204,206,208}Pb$ and $^{32}S + ^{208}Pb$ by using the universal fusion function (UFF) prescription. Then for these reactions, the dynamic effects will be analyzed by the ECC model mentioned above. Finally for the two reactions $^{32}S + ^{204}Pb$ and $^{32}S + ^{206}Pb$, the fusion cross sections at energies near and above the Coulomb barrier will be predicted.

The paper is organized as follows. In Sec. II, we briefly introduce the UFF prescription and the ECC model. In Sec. III, the UFF prescription and the ECC model are applied to analyze the fusion excitation functions of $^{32,34,36}S + ^{204,206,208}Pb$. Finally, a summary is given in Sec. IV.

II. CALCULATION METHODS

A. The universal fusion function

The fusion excitation function is influenced by two types of natures which are associated with the structure of and the interaction of the colliding nuclei. One is the static feature which includes the geometrical aspects, such as the height, radius, and curvature of the barrier and the static effects related to the excess protons or neutrons in weakly bound nuclei. The other one is the dynamic effects of couplings to inelastic excitation channels, nucleon transfer channels, and breakup channels. In order to clearly study the dynamic effects on fusion cross sections of different systems, one way is to completely eliminate the geometrical factors and static effects of the interaction between the projectile and the target. In the present paper, we use the reduction method proposed by Canto *et al.* [64,65] to completely eliminate the geometrical factors and static effects. According to this reduction procedure, the collision energy and the fusion cross sections are reduced to a dimensionless variable x and a dimensionless fusion function $F(x)$,

$$x = \frac{E_{\rm c.m.} - V_{\rm B}}{\hbar\omega}, \qquad F(x) = \frac{2E_{\rm c.m.}}{R_{\rm B}^2\hbar\omega}\sigma_{\rm f}, \tag{1}$$

where $E_{\rm c.m.}$ is the collision energy in the center-of-mass frame and $\sigma_{\rm f}$ denotes the fusion cross section. $R_{\rm B}$, $V_{\rm B}$, and $\hbar\omega$ are the radius, height, and curvature of the barrier when the barrier is replaced by a parabola.

The reduction method shown in Eq. (1) is suggested by Wong's formula [66] for calculating the fusion cross sections,

$$\sigma_{\rm f}^{\rm W}(E_{\rm c.m.}) = \frac{R_{\rm B}^2\hbar\omega}{2E_{\rm c.m.}} \ln\left[1 + \exp\left(\frac{2\pi(E_{\rm c.m.} - V_{\rm B})}{\hbar\omega}\right)\right]. \tag{2}$$

In the case of reaction systems for which the fusion cross section can be accurately described by Wong's formula, then the fusion function $F(x)$ reduces to

$$F_0(x) = \ln[1 + \exp(2\pi x)], \tag{3}$$

$F_0(x)$ is a general function of the variable x and independence of the reaction system. For this reason, $F_0(x)$ is called by the UFF. According to this reduction method, the reduced fusion data of the different reaction systems can be compared directly. The differences between the reduced fusion data of the different reaction systems and the UFF, if exist, are exclusively attributed to the dynamic effects. Thus, the UFF can be used as a uniform standard to study the effects of couplings to inelastic excitation channels and PQNT channels.

B. The empirical coupled-channel model

The fusion cross section at a given center-of-mass energy $E_{\rm c.m.}$ is calculated as the sum of the fusion cross section for each partial-wave J,

$$\sigma_{\rm f}(E_{\rm c.m.}) = \frac{\pi\hbar^2}{2\mu E_{\rm c.m.}} \sum_{J=0}^{J_{\rm max}} (2J+1) T(E_{\rm c.m.}, J), \tag{4}$$

where μ denotes the reduced mass of the reaction system and $J_{\rm max}$ is the critical angular momentum: When the angular momentum J of a partial wave is larger than $J_{\rm max}$, the "pocket" of the potential disappears. T denotes the penetration probability of the potential barrier at a given J.

In the present ECC model, a barrier weight function $f(B)$ is introduced to effectively take into consideration the coupled-channel effects in an empirical way. Thus, the total penetration probability is averaged over the barrier height B and can be calculated as [62,67,68]

$$T(E_{\rm c.m.}, J) = \int f(B) T_{\rm B}(E_{\rm c.m.}, J, B) dB. \tag{5}$$

If one assumes that the potential barrier can be replaced by an "inverted" parabola, the penetration probability $T_{\rm B}$ can be

calculated by the well-known Hill-Wheeler formula [69],

$$T_{\mathrm{B}}^{\mathrm{HW}}(E_{\mathrm{c.m.}}, J, B) = \left\{1 + \exp\left[\frac{2\pi}{\hbar\omega(J)}\left(\frac{\hbar^2 J(J+1)}{2\mu R_{\mathrm{B}}^2(J)} + B - E_{\mathrm{c.m.}}\right)\right]\right\}^{-1}, \quad (6)$$

with B being the barrier height and $\hbar\omega(J)$ and $R_{\mathrm{B}}(J)$ denoting the curvature and the position of the barrier for the Jth partial wave, respectively.

The barrier weight function $f(B)$ is taken to be an asymmetric Gaussian form

$$f(B) = \frac{1}{N}\begin{cases}\exp\left[-\left(\frac{B-B_{\mathrm{m}}}{\Delta_1}\right)^2\right], & B < B_{\mathrm{m}},\\ \exp\left[-\left(\frac{B-B_{\mathrm{m}}}{\Delta_2}\right)^2\right], & B > B_{\mathrm{m}},\end{cases} \quad (7)$$

where Δ_1, Δ_2, and B_{m} denote the left width, the right width, and the most probable value of the barrier weight function, respectively. $f(B)$ satisfies the normalization condition $\int f(B)dB = 1$, hence, the normalization coefficient $N = \sqrt{\pi}(\Delta_1 + \Delta_2)/2$.

When the colliding nuclei come close enough to each other, the two nuclei are distorted because of the repulsive Coulomb force and the attractive nuclear force, the dynamic deformation develops. After taking into account the dynamic deformation, a two-dimensional potential-energy surface with respect to relative distance R and quadrupole deformation of the reaction system can be obtained. Then empirical formulas for calculating Δ_1, Δ_2, and B_{m} have been proposed in our previous work [62]. Moreover, the effect of coupling to PQNT channels is simulated by broadening the empirical barrier weight function, that is, when $Q(2n)$ is positive, the widths $\Delta_i(i = 1, 2)$ of the barrier weight function are changed to $gQ(2n) + \Delta_i(i = 1, 2)$. g is taken to be 0.32 for all reactions with positive $Q(2n)$. In addition, this ECC model has been extended to describe the complete fusion cross sections for reactions involving weakly bound nuclei [70]. More details for the present ECC model can be found in Ref. [62].

III. RESULTS AND DISCUSSIONS

The dynamic effects play a key role to interpret the enhancement of fusion cross sections at sub-barrier energies. In this section, we will first investigate the dynamic effects on fusion cross sections by the UFF prescription. Then, the ECC model is used to analyze the effects of couplings to inelastic excitation channels and PQNT channels.

A. Reduced fusion excitation function

The reduced fusion functions $F(x)$s of the reactions $^{34}\mathrm{S} + ^{204,206,208}\mathrm{Pb}$ and $^{36}\mathrm{S} + ^{204,206,208}\mathrm{Pb}$ are illustrated in Fig. 1. The solid line represents the UFF. The three parameters R_{B}, V_{B}, and $\hbar\omega$ used in the reduction procedure are calculated by the double folding and parameter-free São Paulo potential [73–75], which are listed in Table II. It can be seen that, at the $x < 0$ region, i.e., at energies below the Coulomb barrier, the $F(x)$s of $^{34}\mathrm{S} + ^{204,206,208}\mathrm{Pb}$ and $^{36}\mathrm{S} + ^{204,206,208}\mathrm{Pb}$ are enhanced as compared with the UFF. These enhancements

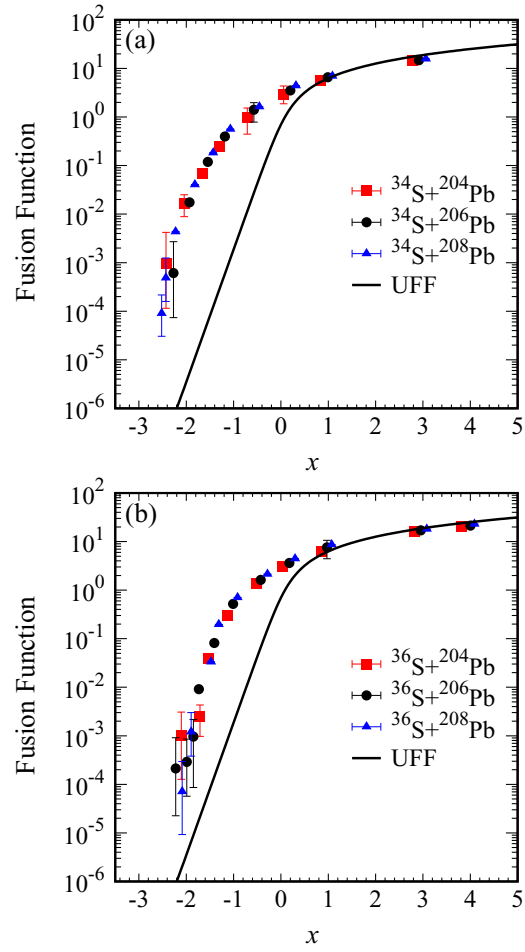

FIG. 1. The reduced fusion excitation functions $F(x)$s for reactions (a) $^{34}\mathrm{S} + ^{204,206,208}\mathrm{Pb}$ and (b) $^{36}\mathrm{S} + ^{204,206,208}\mathrm{Pb}$ as a function of x. The solid line represents the UFF. The experimental data are taken from Ref. [63].

mainly arise from the dynamic effects. It should be noted that, at energies above the Coulomb barrier, there are almost no differences between the $F(x)$s and the UFF for $^{34}\mathrm{S} + ^{204,206,208}\mathrm{Pb}$ and $^{36}\mathrm{S} + ^{204,206,208}\mathrm{Pb}$. This indicates that the dynamic effects in these reactions mainly affect the sub-barrier fusion

TABLE II. The barrier parameters used to reduce the fusion excitation functions.

Reaction	V_{B} (MeV)	$\hbar\omega$ (MeV)	R_{B} (fm)
$^{32}\mathrm{S} + ^{204}\mathrm{Pb}$	146.739	4.573	12.073
$^{32}\mathrm{S} + ^{206}\mathrm{Pb}$	146.413	4.561	12.102
$^{32}\mathrm{S} + ^{208}\mathrm{Pb}$	146.090	4.550	12.131
$^{34}\mathrm{S} + ^{204}\mathrm{Pb}$	145.593	4.430	12.177
$^{34}\mathrm{S} + ^{206}\mathrm{Pb}$	145.272	4.419	12.206
$^{34}\mathrm{S} + ^{208}\mathrm{Pb}$	144.955	4.408	12.235
$^{36}\mathrm{S} + ^{204}\mathrm{Pb}$	144.511	4.300	12.276
$^{36}\mathrm{S} + ^{206}\mathrm{Pb}$	144.195	4.289	12.306
$^{36}\mathrm{S} + ^{208}\mathrm{Pb}$	143.883	4.278	12.334

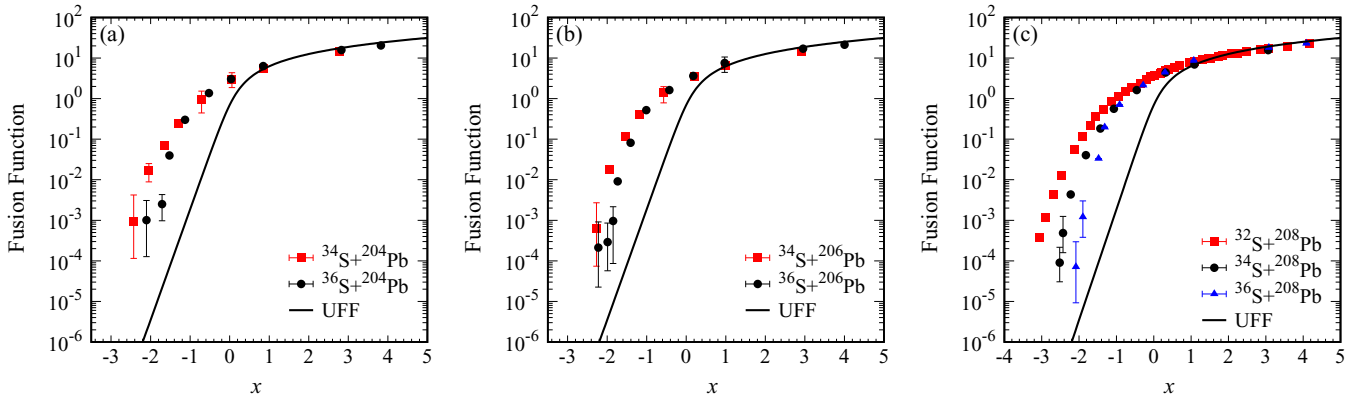

FIG. 2. The reduced fusion excitation functions $F(x)$s for reactions (a) $^{34,36}\mathrm{S}+{}^{204}\mathrm{Pb}$, (b) $^{34,36}\mathrm{S}+{}^{206}\mathrm{Pb}$, and (c) $^{32,34,36}\mathrm{S}+{}^{208}\mathrm{Pb}$ as a function of x. The solid line represents the UFF. The experimental data are taken from Refs. [63,71,72].

cross sections. Furthermore, for the same projectile ^{34}S or ^{36}S on the targets with different isotopes ^{204}Pb, ^{206}Pb, and ^{208}Pb, one can find that the $F(x)$s are consistent with each other. This means that the dynamic effects in the reactions $^{34}\mathrm{S}+{}^{204,206,208}\mathrm{Pb}$ are almost the same. The situation is the same for the reactions with ^{36}S as the projectile.

In addition, it seems that the enhancement of the reactions with ^{34}S as the projectile is a little larger than that of the reactions with ^{36}S as the projectile. To show clearly the enhancements of ^{34}S and ^{36}S on the same target, the $F(x)$s for ^{34}S and ^{36}S on the same target are compared and shown in Fig. 2. One can find that, at the sub-barrier region, the $F(x)$ of the reaction $^{34}\mathrm{S}+{}^{204}\mathrm{Pb}$ is really a little larger than that of the reaction $^{36}\mathrm{S}+{}^{204}\mathrm{Pb}$. The same situations are found in the reactions $^{34,36}\mathrm{S}+{}^{206}\mathrm{Pb}$ and $^{34,36}\mathrm{S}+{}^{208}\mathrm{Pb}$. It indicates that the dynamic effects in reactions with ^{34}S are slightly stronger.

As mentioned above, the larger enhancement of $^{34}\mathrm{S}+{}^{204,206,208}\mathrm{Pb}$ was explained by a stronger coupling to the vibrational states in the reactions with ^{34}S as the projectile in Ref. [63]. It seems that this larger enhancement may be related to the coupling to PQNT channels as the $Q(2n)$s for $^{34}\mathrm{S}+{}^{204,206,208}\mathrm{Pb}$ are positive but negative for $^{36}\mathrm{S}+{}^{204,206,208}\mathrm{Pb}$, which are displayed in Table I. Furthermore, the $F(x)$ of the reaction $^{32}\mathrm{S}+{}^{208}\mathrm{Pb}$ with an even larger $Q(2n)$ is also shown in panel (c) of Fig. 2. As expected, one can see that the $F(x)$ of $^{32}\mathrm{S}+{}^{208}\mathrm{Pb}$ shows an extra enhancement as compared to that of the reaction $^{34}\mathrm{S}+{}^{208}\mathrm{Pb}$. Next, for reactions $^{32,34,36}\mathrm{S}+{}^{204,206,208}\mathrm{Pb}$, the effects of couplings to inelastic excitation channels and neutron transfer channels are evaluated separately by using the ECC model.

B. Calculations with the ECC model

Noted that, in the present ECC model, the parameters of the Coulomb potential and the deformed nuclear potential as well as the empirical formulas for calculating the parameters of the barrier weight function have been fixed. Therefore, there are no free parameters in the following calculations.

First for the reactions with ^{36}S as the projectile are investigated by using the ECC model as the $Q(2n)$s of these reactions are negative. The comparisons of the calculated fusion cross sections and the data are shown in Fig. 3. The solid line denotes the results from the ECC model. It can be seen that the experimental data are reproduced well. This indicates that the effect of coupling to inelastic excitation channels in the reactions $^{36}\mathrm{S}+{}^{204,206,208}\mathrm{Pb}$ is described well.

Next for reactions $^{34}\mathrm{S}+{}^{204,206,208}\mathrm{Pb}$ with positive $Q(2n)$s, the results from the ECC calculations with and without the coupling to PQNT channels considered are shown by the

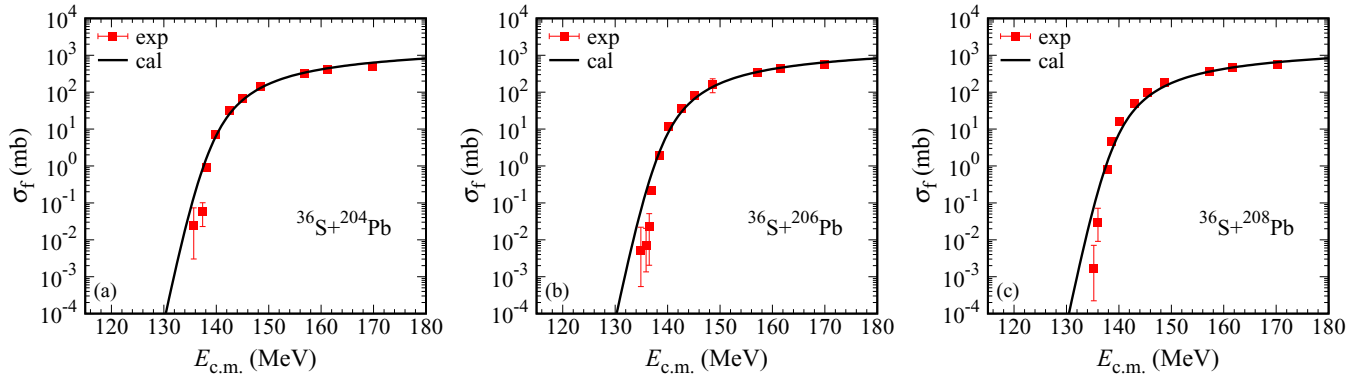

FIG. 3. The calculated and experimental fusion cross sections for reactions $^{36}\mathrm{S}+{}^{204,206,208}\mathrm{Pb}$. The solid line denotes the calculated fusion cross sections from the ECC model. The experimental data are taken from Ref. [63].

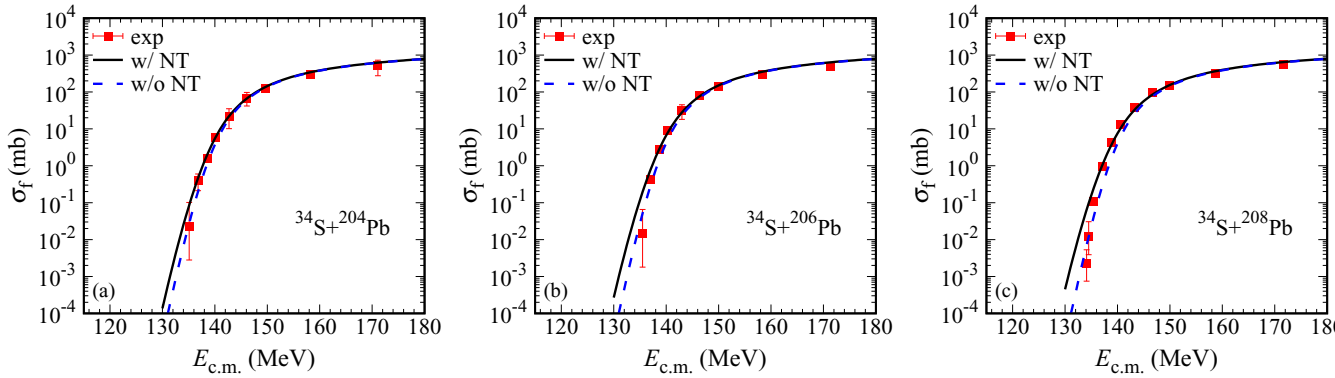

FIG. 4. The fusion cross sections for reactions $^{34}\mathrm{S}+^{204,206,208}\mathrm{Pb}$. The solid lines represent the calculated fusion cross sections from the ECC calculations with the coupling to NT channels considered. The dashed lines are the results from the ECC calculations without the coupling to NT channels considered. The experimental data are taken from Ref. [63].

solid lines and the dashed lines in Fig. 4, respectively. One can see that the measured fusion cross sections can be well reproduced no matter whether the coupling to PQNT channels is considered or not. This implies that the effect of coupling to PQNT channels in these reactions can be neglected. The reason may arise from the fact that the changes in the widths of the barrier weight function, owing to the small $Q(2n)$, are relatively small.

As mentioned above, the $F(x)$ of $^{32}\mathrm{S}+^{208}\mathrm{Pb}$ shows an extra enhancement as compared to that of the reaction $^{34}\mathrm{S}+^{208}\mathrm{Pb}$. This extra enhancement in reaction $^{32}\mathrm{S}+^{208}\mathrm{Pb}$ may come from the coupling to the two-neutron transfer channel with an even larger $Q(2n)$. Then the results from the ECC calculations with and without the coupling to PQNT channels considered are shown by the solid line and the dashed line in panel (c) of Fig. 5, respectively. In this case, one can find that the effect of coupling to PQNT channels is significant and necessary to reproduce the data. It is interesting to note that, for $^{32}\mathrm{S}+^{204}\mathrm{Pb}$ and $^{32}\mathrm{S}+^{206}\mathrm{Pb}$, the $Q(2n)$s are also considerably large (about 5 MeV). Then the predictions of the fusion cross sections for these two reactions are shown in Fig. 5. The solid lines denote the results with the coupling to neutron transfer channels considered. The results without taking into account the coupling to the neutron transfer channels are represented by the dashed lines. It can be seen that the effect of coupling to PQNT channels in these two reactions are also significant. We expect further measurements of fusion cross sections for these two reactions $^{32}\mathrm{S}+^{204}\mathrm{Pb}$ and $^{32}\mathrm{S}+^{206}\mathrm{Pb}$.

IV. SUMMARY

To summarize, the UFF prescription and the ECC model are applied to study the dynamic effects on fusion cross sections for reactions $^{32,34,36}\mathrm{S}+^{204,206,208}\mathrm{Pb}$. The reduced fusion functions show that the total dynamic effects on fusion cross sections for $^{36}\mathrm{S}+^{204,206,208}\mathrm{Pb}$ are almost the same as those for $^{34}\mathrm{S}+^{204,206,208}\mathrm{Pb}$. Furthermore, at sub-barrier energies of the reactions $^{32,34,36}\mathrm{S}+^{208}\mathrm{Pb}$, the largest enhancement of reduced fusion function is observed in the reaction $^{32}\mathrm{S}+^{208}\mathrm{Pb}$. The enhancements of fusion cross sections due to couplings to inelastic excitation channels and neutron transfer channels with positive Q values are analyzed by using the ECC model. The results show that the experimental data of the reactions $^{34,36}\mathrm{S}+^{204,206,208}\mathrm{Pb}$ and $^{32}\mathrm{S}+^{208}\mathrm{Pb}$ are reproduced well by the ECC model. In addition, it can be found that the effect of coupling to positive Q-value neutron transfer channels is necessary to reproduce the sub-barrier fusion data of the reaction $^{32}\mathrm{S}+^{208}\mathrm{Pb}$. Moreover, for the two reactions

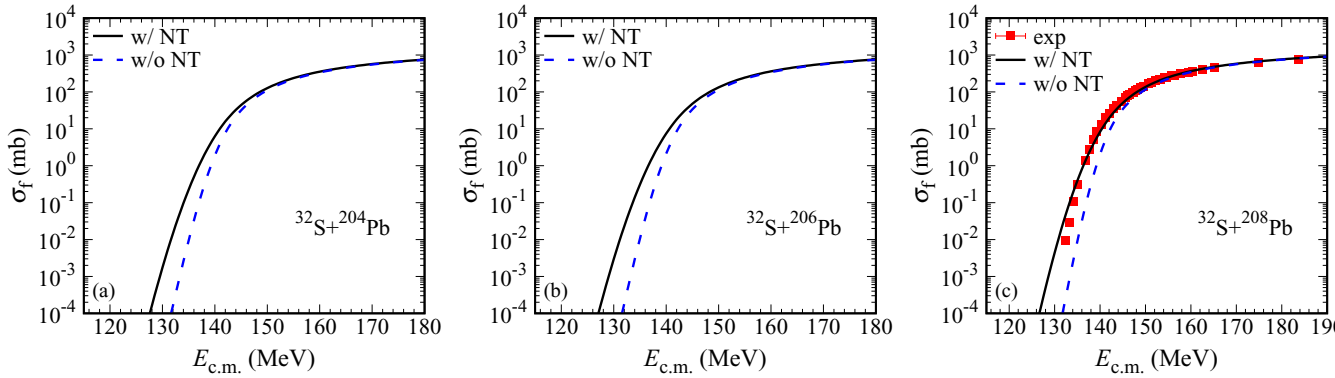

FIG. 5. The calculated fusion cross sections with the ECC model for reactions $^{32}\mathrm{S}+^{204}\mathrm{Pb}$, $^{32}\mathrm{S}+^{206}\mathrm{Pb}$, and $^{32}\mathrm{S}+^{208}\mathrm{Pb}$. The solid lines represent the calculated fusion cross sections from the ECC calculations with the coupling to NT channels considered. The dashed lines are the results from the ECC calculations without the coupling to NT channels considered. The experimental data are taken from Refs. [71,72].

$^{32}S + ^{204}Pb$ and $^{32}S + ^{206}Pb$, the effects of coupling to positive Q-value neutron transfer channels are predicted to be significant. The fusion cross sections for these two reactions are also predicted.

ACKNOWLEDGMENTS

This work has been partly supported by the National Natural Science Foundation of China (Grants No. 11705165, No. 11975209, and No. 11975210).

[1] K. Hagino and N. Takigawa, Prog. Theor. Phys. **128**, 1061 (2012).
[2] B. B. Back, H. Esbensen, C. L. Jiang, and K. E. Rehm, Rev. Mod. Phys. **86**, 317 (2014).
[3] G. G. Adamian, N. V. Antonenko, and W. Scheid, Nucl. Phys. A **618**, 176 (1997).
[4] G. G. Adamian, N. V. Antonenko, W. Scheid, and V. V. Volkov, Nucl. Phys. A **633**, 409 (1998).
[5] G. G. Adamian, N. V. Antonenko, and Y. M. Tchuvil'Sky, Phys. Lett. B **451**, 289 (1999).
[6] G. N. Knyazheva, E. M. Kozulin, R. N. Sagaidak, A. Y. Chizhov, M. G. Itkis, N. A. Kondratiev, V. M. Voskressensky, A. M. Stefanini, B. R. Behera, L. Corradi, E. Fioretto, A. Gadea, A. Latina, S. Szilner, M. Trotta, S. Beghini, G. Montagnoli, F. Scarlassara, F. Haas, N. Rowley *et al.*, and Phys. Rev. C **75**, 064602 (2007).
[7] N. Wang, E.-G. Zhao, W. Scheid, and S.-G. Zhou, Phys. Rev. C **85**, 041601(R) (2012).
[8] N. Wang, E. Zhao, and S.-G. Zhou, J. Phys.: Conf. Ser. **515**, 012022 (2014).
[9] J. Zhang, C. Wang, and Z. Ren, Nucl. Phys. A **909**, 36 (2013).
[10] J. Shen and C. Shen, Sci. China: Phys., Mech. Astron. **57**, 453 (2014).
[11] L. Guo, C. Shen, C. Yu, and Z. Wu, Phys. Rev. C **98**, 064609 (2018).
[12] B. Wang, Z.-Y. Yue, and W.-J. Zhao, Phys. Rev. C **103**, 034605 (2021).
[13] X.-J. Lv, Z.-Y. Yue, W.-J. Zhao, and B. Wang, Phys. Rev. C **103**, 064616 (2021).
[14] G. G. Adamian, N. V. Antonenko, H. Lenske, L. A. Malov, and S.-G. Zhou, Eur. Phys. J. A **57**, 89 (2021).
[15] Y. T. Oganessian and V. K. Utyonkov, Rep. Prog. Phys. **78**, 036301 (2015).
[16] L. Canto, P. Gomes, R. Donangelo, J. Lubian, and M. Hussein, Phys. Rep. **596**, 1 (2015).
[17] C. L. Jiang, H. Esbensen, K. E. Rehm, B. B. Back, R. V. F. Janssens, J. A. Caggiano, P. Collon, J. Greene, A. M. Heinz, D. J. Henderson, I. Nishinaka, T. O. Pennington, and D. Seweryniak, Phys. Rev. Lett. **89**, 052701 (2002).
[18] Ş. Mişicu and H. Esbensen, Phys. Rev. Lett. **96**, 112701 (2006).
[19] M. Dasgupta, D. J. Hinde, A. Diaz-Torres, B. Bouriquet, C. I. Low, G. J. Milburn, and J. O. Newton, Phys. Rev. Lett. **99**, 192701 (2007).
[20] A. Diaz-Torres, D. J. Hinde, M. Dasgupta, G. J. Milburn, and J. A. Tostevin, Phys. Rev. C **78**, 064604 (2008).
[21] T. Ichikawa, K. Hagino, and A. Iwamoto, Phys. Rev. Lett. **103**, 202701 (2009).
[22] V. Y. Denisov, Phys. Rev. C **89**, 044604 (2014).
[23] M. Beckerman, M. Salomaa, A. Sperduto, H. Enge, J. Ball, A. DiRienzo, S. Gazes, Y. Chen, J. D. Molitoris, and Mao Naifeng, Phys. Rev. Lett. **45**, 1472 (1980).
[24] R. A. Broglia, C. H. Dasso, S. Landowne, and A. Winther, Phys. Rev. C **27**, 2433 (1983).
[25] R. A. Broglia, C. H. Dasso, S. Landowne, and G. Pollarolo, Phys. Lett. B **133**, 34 (1983).
[26] P. H. Stelson, H. J. Kim, M. Beckerman, D. Shapira, and R. L. Robinson, Phys. Rev. C **41**, 1584 (1990).
[27] C. H. Dasso, S. Landowne, and A. Winther, Nucl. Phys. A **405**, 381 (1983).
[28] C. H. Dasso, S. Landowne, and A. Winther, Nucl. Phys. A **407**, 221 (1983).
[29] G. L. Zhang, X. X. Liu, and C. J. Lin, Phys. Rev. C **89**, 054602 (2014).
[30] B. Wang, W.-J. Zhao, P. R. S. Gomes, E.-G. Zhao, and S.-G. Zhou, Phys. Rev. C **90**, 034612 (2014).
[31] P. R. S. Gomes, R. Linares, J. Lubian, C. C. Lopes, E. N. Cardozo, B. H. F. Pereira, and I. Padron, Phys. Rev. C **84**, 014615 (2011).
[32] V. V. Sargsyan, G. G. Adamian, N. V. Antonenko, W. Scheid, and H. Q. Zhang, Phys. Rev. C **86**, 054610 (2012).
[33] L. R. Gasques, D. J. Hinde, M. Dasgupta, A. Mukherjee, and R. G. Thomas, Phys. Rev. C **79**, 034605 (2009).
[34] M. Dasgupta, L. R. Gasques, D. H. Luong, R. du Rietz, R. Rafiei, D. J. Hinde, C. J. Lin, M. Evers, and A. Diaz-Torres, Nucl. Phys. A **834**, 147c (2010).
[35] H. Q. Zhang, C. J. Lin, F. Yang, H. M. Jia, X. X. Xu, Z. D. Wu, F. Jia, S. T. Zhang, Z. H. Liu, A. Richard, and C. Beck, Phys. Rev. C **82**, 054609 (2010).
[36] H. M. Jia, C. J. Lin, F. Yang, X. X. Xu, H. Q. Zhang, Z. H. Liu, Z. D. Wu, L. Yang, N. R. Ma, P. F. Bao, and L. J. Sun, Phys. Rev. C **89**, 064605 (2014).
[37] H. Timmers, D. Ackermann, S. Beghini, L. Corradi, J. H. He, G. Montagnoli, F. Scarlassara, A. M. Stefanini, and N. Rowley, Nucl. Phys. A **633**, 421 (1998).
[38] A. M. Stefanini, B. R. Behera, S. Beghini, L. Corradi, E. Fioretto, A. Gadea, G. Montagnoli, N. Rowley, F. Scarlassara, S. Szilner, and M. Trotta, Phys. Rev. C **76**, 014610 (2007).
[39] R. Pengo, D. Evers, K. E. G. Löbner, U. Quade, K. Rudolph, S. J. Skorka, and I. Weidl, Nucl. Phys. A **411**, 255 (1983).
[40] J. J. Kolata, A. Roberts, A. M. Howard, D. Shapira, J. F. Liang, C. J. Gross, R. L. Varner, Z. Kohley, A. N. Villano, H. Amro, W. Loveland, and E. Chavez, Phys. Rev. C **85**, 054603 (2012).
[41] R. N. Sahoo, M. Kaushik, A. Sood, A. Sharma, S. Thakur, P. Kumar, M. M. Shaikh, R. Biswas, A. Yadav, M. K. Sharma, J. Gehlot, S. Nath, N. Madhavan, R. G. Pillay, E. M. Kozulin, G. N. Knyazheva, K. V. Novikov, and P. P. Singh, Phys. Rev. C **102**, 024615 (2020).
[42] P. Jacobs, Z. Fraenkel, G. Mamane, and I. Tserruya, Phys. Lett. B **175**, 271 (1986).
[43] H. M. Jia, C. J. Lin, F. Yang, X. X. Xu, H. Q. Zhang, Z. H. Liu, L. Yang, S. T. Zhang, P. F. Bao, and L. J. Sun, Phys. Rev. C **86**, 044621 (2012).
[44] V. I. Zagrebaev, Phys. Rev. C **67**, 061601(R) (2003).
[45] V. V. Sargsyan, G. G. Adamian, N. V. Antonenko, W. Scheid, and H. Q. Zhang, Phys. Rev. C **86**, 014602 (2012).

[46] V. V. Sargsyan, G. Scamps, G. G. Adamian, N. V. Antonenko, and D. Lacroix, Phys. Rev. C **88**, 064601 (2013).
[47] V. V. Sargsyan, G. G. Adamian, N. V. Antonenko, W. Scheid, and H. Q. Zhang, Phys. Rev. C **91**, 014613 (2015).
[48] K. Hagino, N. Rowley, and A. L. Kruppa, Comput. Phys. Commun. **123**, 143 (1999).
[49] A. S. Umar and V. E. Oberacker, Phys. Rev. C **74**, 021601(R) (2006).
[50] A. S. Umar, V. E. Oberacker, J. A. Maruhn, and P.-G. Reinhard, Phys. Rev. C **85**, 017602 (2012).
[51] R. Keser, A. S. Umar, and V. E. Oberacker, Phys. Rev. C **85**, 044606 (2012).
[52] L. Guo, J. A. Maruhn, and P.-G. Reinhard, Phys. Rev. C **76**, 014601 (2007).
[53] L. Guo, J. A. Maruhn, P.-G. Reinhard, and Y. Hashimoto, Phys. Rev. C **77**, 041301(R) (2008).
[54] G.-F. Dai, L. Guo, E.-G. Zhao, and S.-G. Zhou, Sci. China: Phys., Mech. Astron. **57**, 1618 (2014).
[55] G.-F. Dai, L. Guo, E.-G. Zhao, and S.-G. Zhou, Phys. Rev. C **90**, 044609 (2014).
[56] N. Wang, Z. Li, and X. Wu, Phys. Rev. C **65**, 064608 (2002).
[57] N. Wang, K. Zhao, and Z. Li, Phys. Rev. C **90**, 054610 (2014).
[58] N. Wang, Z. Li, X. Wu, J. Tian, Y. X. Zhang, and M. Liu, Phys. Rev. C **69**, 034608 (2004).
[59] K. Wen, F. Sakata, Z.-X. Li, X.-Z. Wu, Y.-X. Zhang, and S.-G. Zhou, Phys. Rev. Lett. **111**, 012501 (2013).
[60] K. Wen, F. Sakata, Z.-X. Li, X.-Z. Wu, Y.-X. Zhang, and S.-G. Zhou, Phys. Rev. C **90**, 054613 (2014).
[61] N. Wang, K. Zhao, and Z. Li, Sci. China: Phys., Mech. Astron. **58**, 112001 (2015).
[62] B. Wang, K. Wen, W.-J. Zhao, E.-G. Zhao, and S.-G. Zhou, At. Data Nucl. Data Tables **114**, 281 (2017).
[63] J. Khuyagbaatar, K. Nishio, S. Hofmann, D. Ackermann, M. Block, S. Heinz, F. P. Heßberger, K. Hirose, H. Ikezoe, B. Kinlder, B. Lommel, H. Makii, S. Mitsuoka, I. Nishinaka, T. Ohtsuki, Y. Wakabayashi, and S. Yan, Phys. Rev. C **86**, 064602 (2012).
[64] L. F. Canto, P. R. S. Gomes, J. Lubian, L. C. Chamon, and E. Crema, J. Phys. G: Nucl. Phys. **36**, 015109 (2009).
[65] L. F. Canto, P. R. S. Gomes, J. Lubian, L. C. Chamon, and E. Crema, Nucl. Phys. A **821**, 51 (2009).
[66] C. Y. Wong, Phys. Rev. Lett. **31**, 766 (1973).
[67] B. Wang, W. Zhao, E. Zhao, and S. Zhou, Sci. China: Phys., Mech. Astron. **59**, 642002 (2016).
[68] B. Wang, W.-J. Zhao, E.-G. Zhao, and S.-G. Zhou, Phys. Rev. C **98**, 014615 (2018).
[69] D. L. Hill and J. A. Wheeler, Phys. Rev. **89**, 1102 (1953).
[70] B. Wang, W.-J. Zhao, A. Diaz-Torres, E.-G. Zhao, and S.-G. Zhou, Phys. Rev. C **93**, 014615 (2016).
[71] M. Dasgupta and D. Hinde, Nucl. Phys. A **734**, 148 (2004).
[72] D. J. Hinde, M. Dasgupta, N. Herrald, R. G. Neilson, J. O. Newton, and M. A. Lane, Phys. Rev. C **75**, 054603 (2007).
[73] M. A. Cândido Ribeiro, L. C. Chamon, D. Pereira, M. S. Hussein, and D. Galetti, Phys. Rev. Lett. **78**, 3270 (1997).
[74] L. C. Chamon, D. Pereira, M. S. Hussein, M. A. Cândido Ribeiro, and D. Galetti, Phys. Rev. Lett. **79**, 5218 (1997).
[75] L. C. Chamon, B. V. Carlson, L. R. Gasques, D. Pereira, C. De Conti, M. A. G. Alvarez, M. S. Hussein, M. A. Cândido Ribeiro, E. S. Rossi, and C. P. Silva, Phys. Rev. C **66**, 014610 (2002).